ARTICLE OPEN

Aberrant lipid metabolism renders an aggressive behavior of T-lymphoblastic lymphoma in a MASH model

Wei Guo[1,2], Xingtong Wang[1,2], Guozhen Cui[3], Emily A. S. Schmieder[1], Yonglin Gao[1], Butian Zhang[4], Robert C. G. Martin[1], Ou Bai[2]✉ and Yan Li[1]✉

Liver involvement of lymphomas is not rare in clinical patients. Metabolic dysfunction-associated steatohepatitis (MASH, formerly known as nonalcoholic steatohepatitis) is well accepted as a potential precursor for liver cancer, but it is unknown whether MASH could promote extranodal infiltration of lymphoma. In this study, the subpopulation of tumor-initiating cells and Wnt signaling pathway activation were studied in T-lymphoblastic lymphoma cells. Tumor growth, Wnt/β-catenin signaling, and fenofibrate therapy were investigated in an MASH-lymphoma mouse model. We found that up-regulated Wnt/β-catenin and epithelial cell adhesion molecule signaling contributed to aggressive growth of T-lymphoblastic lymphoma in vitro and in vivo. Lack of fibroblast growth factor 21 (FGF21) worsened lipid metabolic disorder in the hepatic microenvironment which further promoted lymphoma growth in the MASH liver. Fenofibrate therapy upregulated the peroxisome proliferator-activated receptor alpha (PPAR-α)-FGF21 axis, thereby alleviated not only MASH but also liver infiltration of T-lymphoblastic lymphoma. In addition, down-regulated FGF21 but up-regulated Wnt signaling was found in T-cell lymphoma patient samples. In conclusion, aberrant lipid metabolism contributed to the aggressive growth of T-lymphoblastic lymphoma cells in MASH liver. Wnt/β-catenin signaling could be a potential lymphomagenetic mechanism for extranodal infiltration of T-lymphoblastic lymphoma. Fenofibrate has the potential to be an effective therapeutic strategy against liver infiltration of T-lymphoblastic lymphoma in MASH liver.

Oncogene (2026) 45:56–67; https://doi.org/10.1038/s41388-025-03630-7

Graphical Abstract

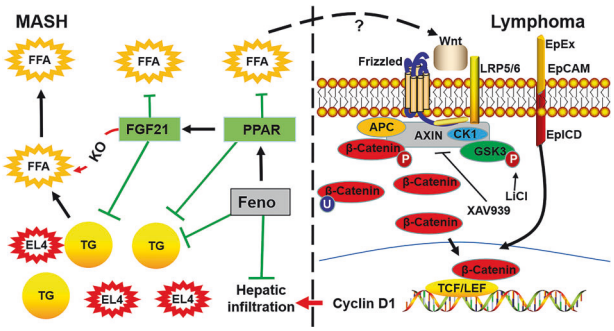

INTRODUCTION

Primary hepatic lymphoma is a clinically rare cancer comprising only 0.016% of all cases of non-Hodgkin's lymphoma (NHL) and 0.4% of extranodal NHL [1]. Despite this, a substantial number of hepatic mucosa-associated lymphoid tissue lymphomas were reported to occur in patients with chronic hepatitis [2–4]. Liver involvement is not rare in lymphoma patients, including diffuse large B-cell lymphoma (DLBCL), Burkitt lymphoma (BL), T-cell lymphomas, marginal zone B-cell lymphomas (MZL), and other lymphoma subtypes [5]. Development of metabolic dysfunction-associated steatohepatitis (MASH) in lymphoma patients is drawing more notice, e.g., MASH has occurred in patients with T-lymphoblastic lymphoma during chemotherapy [6, 7]. In addition, fulminant hepatic failure developed in a woman with stage IV Hodgkin's disease during a short course of prednisone (2 weeks) [8]. In a 1-year cohort study involving 227 lymphoma

[1]Department of Surgery, School of Medicine, University of Louisville, Louisville, KY, USA. [2]Department of Hematology, The First Hospital of Jilin University, Changchun, Jilin, China. [3]Department of Medical Oncology, The First Hospital of Jilin University, Changchun, Jilin, China. [4]Department of Radiology, China-Japan Union Hospital of Jilin University, Changchun, Jilin, China. ✉email: baiou@jlu.edu.cn; yan.li@louisville.edu

Received: 31 January 2025 Revised: 2 October 2025 Accepted: 12 November 2025
Published online: 26 November 2025

patients, hepatic steatosis was observed in 11.9% of the patients during their baseline or post-treatment evaluation [9]. There is mounting evidence revealing a close relationship between MASH and lymphomagenesis, however, it is unknown whether MASH could promote the extranodal infiltration in the liver. As MASH is known to lead to hepatic malignancy, this disease calls for further investigation into its role contributing to lymphomagenesis.

Aberrant Wnt/β-catenin signaling pathways play a crucial role in facilitating the progression of hematological malignancies, including lymphomas [10]. Activation of Wnt/β-catenin signaling is known to endow cancer cells with sustained self-renewing growth, resulting in an increase in tumor-initiating cells and further malignancy in the tumor of origin [11]. In our previous studies, we found that lack of fibroblast growth factor 21 (FGF21), an endocrine FGF primarily produced in the liver [12, 13], could contribute to MASH-hepatocellular carcinoma (HCC) transition via up-regulated Wnt/β-catenin signaling [14, 15]. FGF21 elicits metabolic benefits to protect the liver against MASH via upregulation of lipolysis and clearance of excessive free fatty acids (FFAs), thereby negatively regulating steatosis [12, 13, 16]. Epidemiologic evidence suggests that obesity and increased fat intake, in particular saturated fat, may increase the risk of NHL [17]. Our resent study suggests an aggressive growth behavior of lymphoma cells in obese mice [18].

The aim of this study is to elucidate the mechanistic action of Wnt/β-catenin pathway in hepatic lymphoma and to find potential therapeutic targets. By establishing MASH-lymphoma mouse model via lymphoma cell (EL4) inoculation into the liver lobes, we studied the tumor growth and Wnt signaling in FGF21 knockout mice and wild type controls. To induce peroxisome proliferator-activated receptor alpha (PPAR-α) and FGF21, we used fenofibrate to treat MASH-lymphoma mice to investigate fenofibrate's preventive effect against lymphoma tumor growth in the MASH liver.

MATERIALS AND METHODS

Cell lines and treatments

A murine T lymphocyte (lymphoma) line (EL4, TIB-39), a human T lymphocyte (lymphoma) line (HH, CRL-2105), and a mouse hepatocyte line (FL83B, CRL-2390) were purchased from American Type Culture Collection (ATCC) (Manassas, VA). EL4 cells were cultured in Dulbecco's Modified Eagle's Medium (ATCC, 30–2002) with 10% horse serum (SigmaAldrich, H1270) and Pen/Strep (Corning, 30-002-CI). HH cells were cultured in RPMI-1640 medium (ATCC, 30–2001) and FL83B cells were cultured in F-12K medium (ATCC, 30-2004), supplemented with 10% fetal bovine serum (FBS) (SigmaAldrich, 12103 C) and Pen/Strep. Establishment of FL83B-FGF21KD cell is described in the supplemental file. For fatty acid (FA) treatment, a 2:1 ratio of oleic acid (Sigma-Aldrich, O1383) and palmitic acid (Sigma-Aldrich, P5585) was made in DMEM, established as OP-media to treat EL4 cells, HH cells and FL83B cells. A cell proliferation assay (XTT assay) was performed to determine optimal concentrations for the OP challenging, and 1% BSA was used as the treatment control. The in vitro treatments were the following: rhFGF21 (PeproTech, 100-42) at 100 ng/mL, XAV939 (Abcam, ab120897) at 1 μM, LiCl (Sigma-Aldrich, L9650) at 20 mM, and fenofibrate (Sigma, F6020-5G) at 100 μM. All the antibodies and primers used are listed in the supplemental file.

Animal models

Male FGF21 knockout (FGF21KO) mice with C57 BL/6 J background were generously granted by Dr. Steve Kliewer (University of Texas Southwestern Medical Center). C57BL/6 J (Strain 000664) WT mice were purchased from Jackson Laboratories (Bar Harbor, ME). All animals were housed 4 per cage, given rodent chow and tap water ad libitum, and maintained at 22 °C and on a 12-h light/dark cycle. To establish MASH model, 4-week-old male mice were fed with high fat (60%) methionine- and choline-deficient diet (HFMCD) for 2 weeks, while low fat (10%) diet was used as control diet (CD). To establish the MASH-lymphoma model, a 1.5-cm midline laparotomy incision was made under anesthesia to expose the spleen and EL4 cells suspended in 0.1 ml PBS were injected at a concentration of 1×10^6 cells/injection. The abdominal wall was closed in two layers using 5–0 Vicryl suture (Ethicon, New Brunswick, NJ). By simple, block, stratified, and covariate adaptive randomization, the mice in MASH and MASH-lymphoma model were assigned randomly into each experimental group. Tumor growth was monitored weekly by ultrasound. The mice had bodyweight loss over 20% or ascites were excluded. Mice were euthanized at the end of studies to collect blood, serum, tumor, lymph nodes, liver, and adipose tissues (gonadal, retroperitoneal, and mesenteric) for further analysis. To count macroscopical tumor nodule, left and right liver lobes were sliced sagittally into 6 pieces, 3 pieces for each lob, and recorded as tumor nodules/liver/mouse. For the fenofibrate treatment, MASH-lymphoma mice received fenofibrate peritoneal injections at 100 mg/kg/day for four weeks. All animal procedures were approved by the Institutional Animal Care and Use Committee of the University of Louisville, which is certified by the American Association for Accreditation of Laboratory Animal Care.

Statistical analysis

Collected data from repeated experiments were presented as mean ± SD. For in vitro studies, all experiments were performed with a minimum of triplicate samples and triplicate repetition of experiments. For in vivo studies, six mice were assigned in each group to establish the lymphoma model, and eight mice were assigned in each group for fenofibrate treatment, to detect an effect size of 1.5 with a power of 90% at a significant level of 0.05. Statistical analysis was performed by using GraphPad Prism v7.0. Statistical significance of lymphoma patient samples was determined by an ANOVA, and difference between groups was elucidated by a post hoc Tukey's test. Group differences were considered significant and denoted with $P < 0.05$ (*) and $P < 0.01$(**). A Kaplan–Meier analysis was performed to determine the differences in survival rates using log-rank tests.

RESULTS

FGF21 and Wntβ-catenin pathways in human and mouse T-lymphoblastic lymphoma

A network-based dataset (GSE160119) of 84 natural killer/T-cell lymphoma (NKTL) samples and 4 lymph node control samples [19] were used to analyze the differentially expressed genes (DEGs). Unsupervised clustering identified two distinct subgroups, with the top-ranked 25 DEGs across all lymphoma and lymph node specimens. The heat-map clearly showed the divergent expression patterns of the DEGs in which FGF21 gene was identified as the 18th DEG (Fig. 1A). The DEGs extracted from the full DEG list to further analyze the Wnt pathway-related genes in the 84 lymphoma samples which were sub-grouped into FGF21-high and FGF21-low groups based on the average FGF21 expression level. A heatmap was created to show the selected 11 Wnt-related genes which represented the important components of Wnt signaling including Wnt pathway-associated transcription factors, Wnt pathway positive regulators, and the Wnt pathway inhibitory factors [20, 21]. In most FGF21 low-expression samples, the Wnt pathway-associated transcription factors such as transcription factor 4 (TCF4) and lymphoid enhancer-binding factor 1 (LEF1), as well as Wnt pathway positive regulators like low-density lipoprotein receptor-related protein 5 (LRP5) and LRP6 were upregulated. In contrast, the Wnt pathway inhibitory factors such as adenomatous Polyposis Coli (APC) and glycogen synthase kinase-3β (GSK-3β) were downregulated (Fig. 1B). These results suggested a negative correlation between FGF21 and Wnt signaling pathway. Two standard gene sets (KEGG_WNT_SIGNALING_PATHWAY and GO_WNT_SIGNALING_PATHWAY) were used to further investigate FGF21 signaling and Wnt signaling by Gene Ontology (GO)-based GSEA analysis. The GOChord plot showed that FGF21 was linked mostly to the Wnt signaling pathway and the cell-to-cell signaling by Wnt (Fig. S1A). The GSEA analysis revealed the enriched genes in Wnt signaling pathway and Wnt cell-to-cell signaling pathways, which were closely associated with FGF21 gene expression (Fig. S1B). All these results indicated that both FGF21 and Wnt genes contributed to a systematic

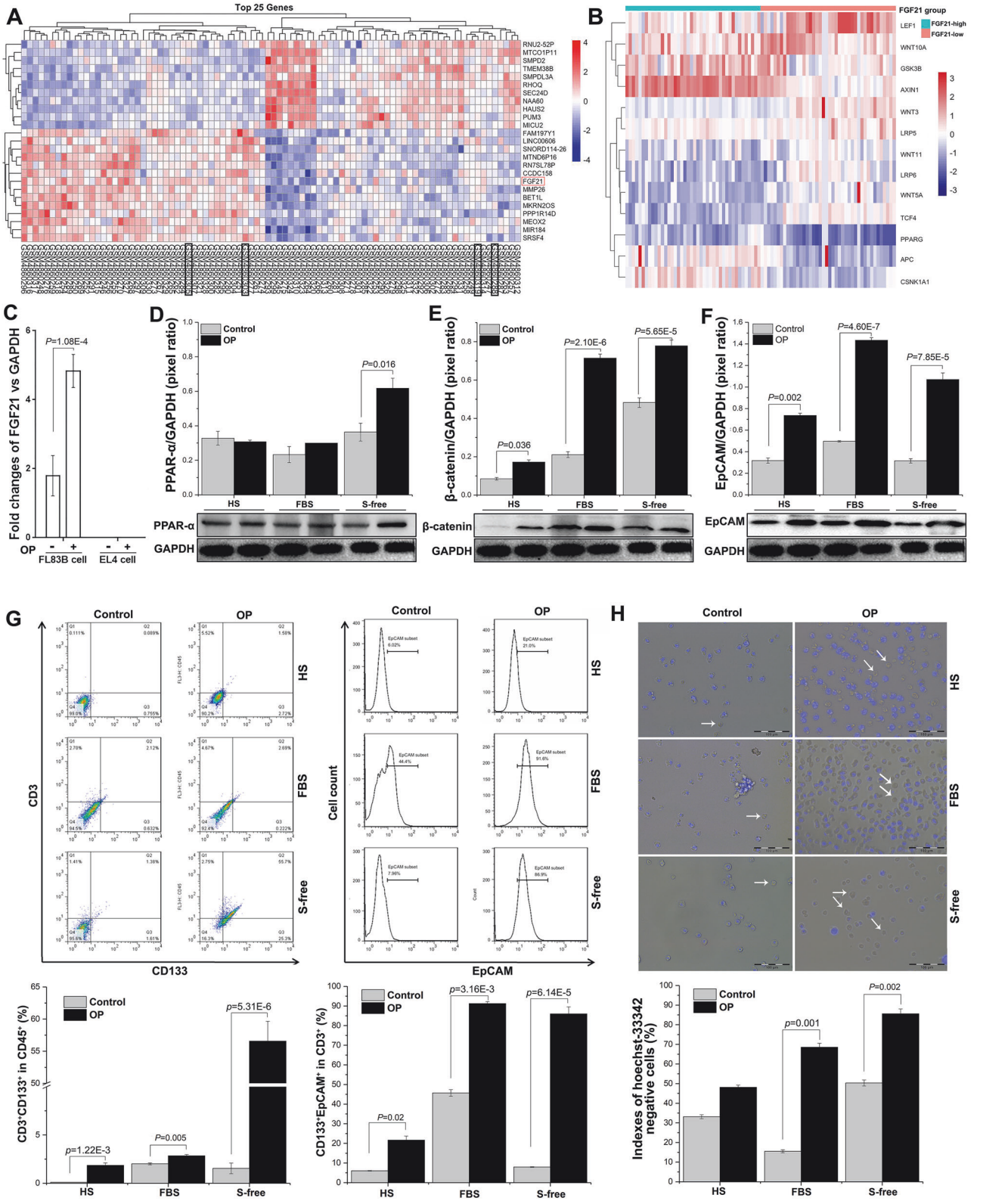

Fig. 1 Bioinformatics analysis and FA induced tumor-initiating subpopulation in mouse T-lymphoblastic lymphoma cells. A Heatmap of DEGs (NKTLs versus lymph node controls) in which FGF21 was identified as the 18th DEG in the top 25 DEGs. Black frame boxes: lymph node control samples. **B** Heatmap to show the Wnt pathway-associated DEGs in the 84 lymphoma samples with high FGF21 expression and with low FGF21 expression. **C** qPCR analysis to detect FGF21 mRNA in the EL4 cells with/without OP challenging. **D–F** Western blotting analysis to detect the protein levels of PPAR-α, β-catenin, and EpCAM in the EL4 cells with/without OP challenging. **G** Flowcytometry analysis to detect the $CD133^{+}EpCAM^{+}$ subpopulation in the EL4 cells with/without OP challenging. **H** Hoechst33342 staining to evaluate the dye-efflux ability in the EL4 cells with/without OP challenging. OP: a mixture of oleic acid and palmitic acid (2:1); HS horse serum, FBS fetal bovine serum, S-free serum-free.

interpretation with functional relevance within a broader biological context.

Because the most important function of FGF21 is to upregulate lipolysis and clear excessive FFA, we therefore investigated the FGF21 signaling and the Wnt pathway in the fatty acid (FA) challenged lymphoma cells. Based on the results of cell viability (Fig. S1C), 0.3 mM OP (mixture of OA and PA at 2:1) was selected to treat the EL4 cells for 24 h, while FL83B cells were used as a positive control for FGF21 expression. Unlike the FL83B cells, the mRNA of FGF21 was not detected by qPCR in the EL4 cells either untreated (UT) or challenged with OP (Fig. 1C). Previous reports indicated that PPAR-α, an upstream signal to induce FGF21 expression [22], was expressed by hematologic malignancies such as chronic lymphocytic leukemia and lymphoma [23]. Interestingly, increased PPAR-α protein levels were found in the EL4 cells challenged by OP (Fig. 1D), suggesting that PPAR-α could be upregulated in EL4 cells even though FGF21 was absent. Significantly upregulated protein expressions of β-catenin (an important component of Wnt signaling) and EpCAM (a potential marker of tumor-initiation) were found in EL4 cells challenged by the media of OP-horse serum (HS), OP-fetal bovine serum (FBS), and OP-serum free (SF), compared to the respective control media (Fig. 1E, F). We next questioned whether an overabundance of FA could act as a possible trigger of lymphomagenesis, in addition to the established role of FA in hepatocellular carcinogenesis [24]. Flowcytometry of EL4 cells showed an increase in the subpopulation of $CD133^{+}EpCAM^{+}$ cells (Fig. 1G) for all three OP-media replicates compared to the control media. Hoechst-33342 staining was performed to evaluate the dye-efflux ability which has been widely accepted as a functional marker of tumor-initiating cells [25]. Numerous Hoechst33342 negative stained EL4 cells were found in the OP-media (Fig. 1H), indicating that oversupplying FA could facilitate EL4 cells acquiring tumor-initiating properties. Taken together, a lack of FGF21 can play an important role in Wnt/β-catenin signaling and subsequent tumor-initiating lymphoma cells [26]. Fatty acid flooding promoted tumor-initiating cell progression which could lead to aggressiveness of lymphoma.

Up-regulated Wnt/β-catenin signaling in FGF21KO-MASH liver

To recapitulate steatohepatitis, we established a MASH model in FGF21KO and wild type (WT) mice by using HFMCD for two weeks [27]. The gross appearance of MASH liver presented as diffusely pale-yellow-tan colored lobes (Fig. S2A) along with an increase in liver weight/body weight and serum alanine aminotransferase levels in the MASH mice (Fig. S2B). Extensively distributed lipid drops were identified by E&H staining in the MASH mice (Fig. 2A). MASH was diagnosed by the histological changes (steatosis, inflammation, and ballooning) and NAFLD Active Score (NAS) [28]. Either WT mice or FGF21KO mice with HFMCD had a high NAS (>5) while the highest NAS was found in the FGF21KO-HFMCD mice (Fig. 2A). The HFMCD induced MASH model was further validated by the MASH model fed with high fat high fructose diet (HFHFD), a western-style diet, for 3 months. There was no statistical significance of NAS between HFMCD model and HFHFD model (Fig. S2C). There was a significant increase in lipid accumulation confirmed by Oil red O staining and triglyceride (TG) levels (in serum and liver tissue) (Fig. 2B–D). A statistically significant increase in serum FFA levels was found in both WT mice and FGF21KO mice fed HFMCD, compared to the controls. The highest FFA level was found in the FGF21KO-MASH mice compared to the other 3 groups (Fig. 2E), suggesting that the lack of hepatic FGF21 not only worsened MASH but also caused excessive FFAs. Acting as a liver safeguard [29], FGF21 is highly expressed and released in response to high glucose and high FFAs [30]. We wondered whether the lack of FGF21 could be a potential microenvironmental factor for activation of β-catenin and EpCAM in the MASH liver. Consistent with serum FFA levels, significantly upregulated protein levels of β-catenin and EpCAM were found in the liver tissues from both WT mice and FGF21KO mice fed with HFMCD, compared to the control mice (Fig. 2F, G). The highest protein levels of β-catenin and EpCAM were found in the FGF21KO-MASH mice (Fig. 2F, G). Taken together, a lack of FGF21 worsened MASH and activated Wnt/β-catenin and EpCAM signaling in the liver.

Aggressive growth of EL4 cells in FGF21KO-MASH liver

To study the growth behavior of lymphoma cells in a MASH liver, we established a hepatic lymphoma model in both WT-MASH and FGF21KO-MASH mice as well as non-MASH lymphoma controls. Orthotopic inoculation was performed by EL4 cell injection. Two weeks after EL4 cell injection, the mice were sacrificed, and the entire liver was harvested to evaluate tumor growth (Fig. 3A). Gross anatomy showed multiple tumor nodules in the liver lobes from the MASH-lymphoma mice (WT and FGF21KO), but significantly less tumor nodules from the non-MASH lymphoma control mice (Fig. 3B). In H&E-stained micro-sections, steatohepatitis was characterized as widely distributed lipid drops and infiltration of inflammatory cells in the acinar zone. Cytologic characteristics of the infiltrated lymphoma cells showed improperly cleaved cells, plasmacytoids, larger in size versus normal lymphocytes with round nuclear outlines, vesicular chromatin, and single to multiple prominent nucleoli (Fig. 3B). Significantly increased tumor nodule counts (Fig. 3C) and positive staining of proliferating cell nuclear antigen (PCNA) (Fig. 3D) were present in the tumor tissue sections from the MASH-lymphoma mice (WT and FGF21KO), compared to the non-MASH lymphoma control mice. Interestingly, a significantly higher number of PCNA-positive cells was found in the tumor tissues from FGF21KO-lymphoma mice compared to the WT-lymphoma mice (Fig. 3D). A dual immunofluorescent staining in frozen tissue sections was performed to confirm tumors origin from the EL4 cells. As expected, $CD3^{+}CD133^{+}$ cells were predominantly distributed in the tumor nodules from all the mice with EL4 cell orthotopic inoculation (Fig. 3E). EL4 cell infiltration in other organs, termed as extranodal infiltration (Ex), was further analyzed by macroscopic observation of tumor nodules in the organs including the stomach, lung, spleen, and skin. In each treatment arm, the mice were grouped as TG^{high} and TG^{low} based on the average serum TG level. We further analyzed the 2 groups of TG^{high} and TG^{low} mice with Ex cases and without Ex cases. Fifty-seven percent of $TG^{high}Ex^{+}$ cases were in the FGF21KO-MASH-lymphoma group, while 43% $TG^{high}Ex^{+}$ cases were the WT-MASH-lymphoma mouse (Fig. 3F), suggesting that the aggressive growth pattern of EL4 cells was positively associated with high serum TG level. Most $TG^{low}Ex^{-}$ cases were found in non-MASH mice (71% in FGF21KO-lymphoma mice and 86% in WT-lymphoma mice), indicating the importance of dyslipidemia contributing to lymphoma Ex (Fig. 3F). Significantly upregulated protein expressions of β-catenin and EpCAM were found in the tumor nodule tissues compared to benign adjacent tissues, while the highest levels of protein productions of β-catenin and EpCAM were found in the tumor nodule tissues from the FGF21KO-MASH-lymphoma mice (Fig. 3G, H). These results suggest that upregulation of Wnt/β-catenin and EpCAM signaling played a promoting role in lymphomagenesis, in turn to accelerating tumor growth and Ex. In addition, the absence of FGF21 had an impact on not only lipid metabolism but also Wnt/β-catenin and EpCAM signaling. A shRNA assay was performed to knockdown (KD) the expression of FGF21 gene in FL83B cells to further investigate the role of FGF21 on Wnt/β-catenin and EpCAM signaling. By OP challenging, only a slight increase of FGF21 protein was found in the FL83B-21KD cells compared to FL83B-shCT (control) cells (Fig. S3A), suggesting the success of FGF21 gene knockdown. To study the crosstalk between hepatocytes and EL4 cells, EL4 cells were co-cultured with FL83B-21KD cells and FL83B-shCT cells with/without OP challenging. Significantly increased protein expressions of β-catenin and EpCAM were found in the EL4 cells co-cultured with the OP-challenged FL83B-

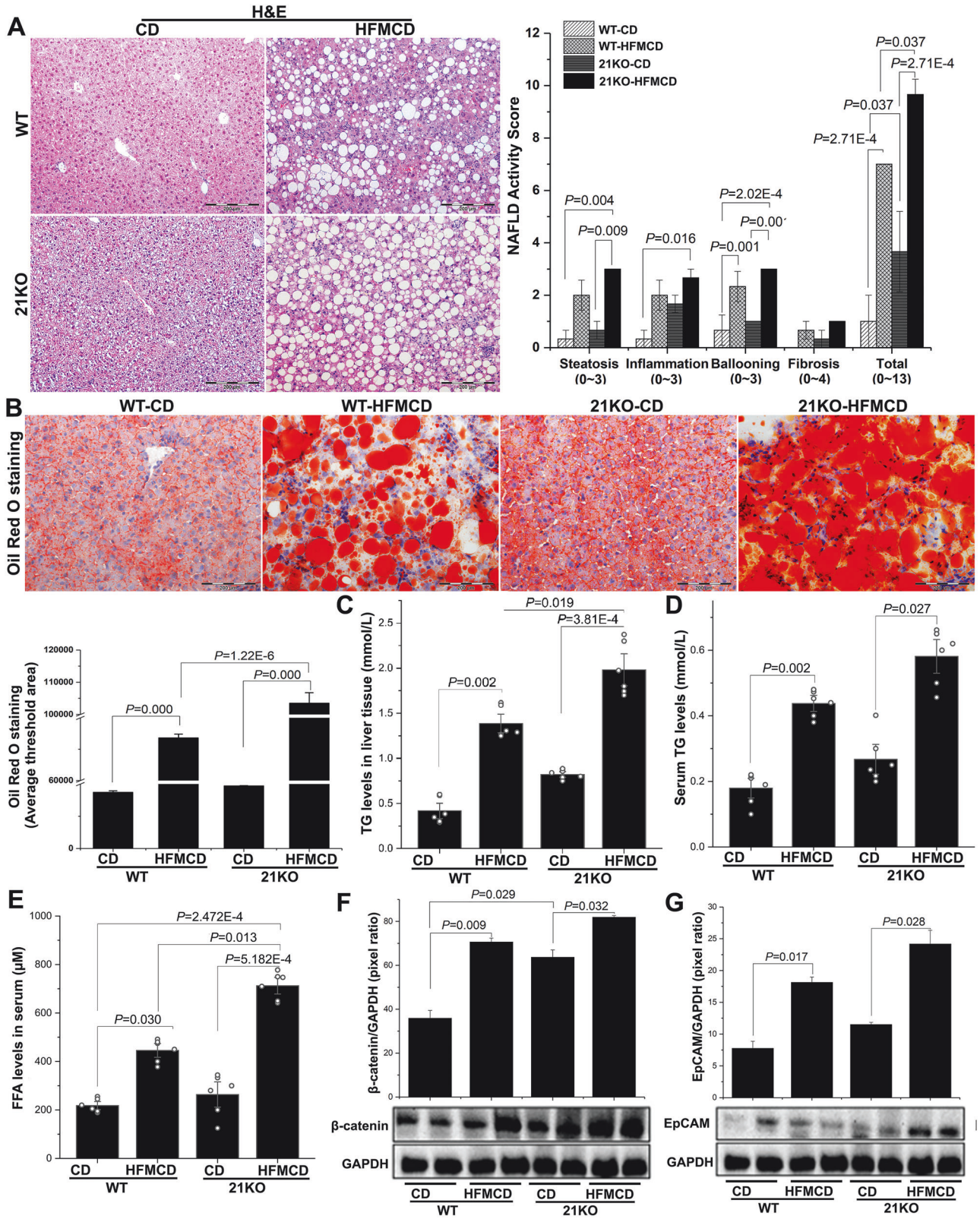

Fig. 2 Up-regulated Wnt/β-catenin signaling in FGF21KO-MASH liver. A Representative histology by H&E staining and the histology based NAFLD activity score (NAS) from MASH mice and controls. **B** Lipid accumulation detected by Oil Red O staining along with computer-imaging analysis in the liver tissue slides from MASH mice and controls. **C**, **D** TG levels in liver tissue and in serum from MASH mice and controls. **E** Serum FFA levels in MASH mice and controls. **F**, **G** Western blotting analysis to detect the protein levels of β-catenin and EpCAM in the liver tissues from MASH mice and controls. Animal number (n) = 6 in each group; 21KO: FGF21KO.

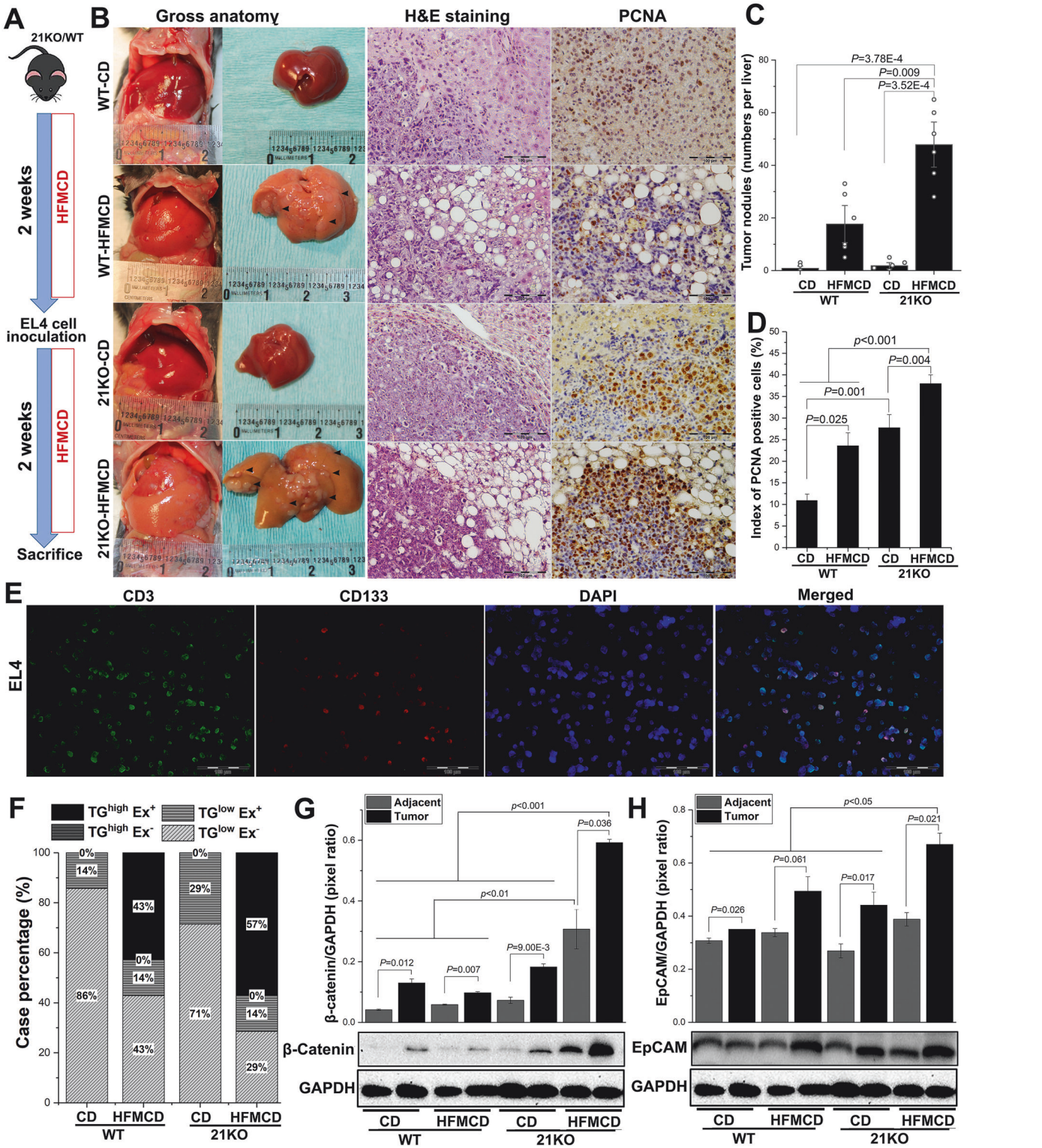

Fig. 3 Aggressive growth of EL4 cells in FGF21KO-MASH liver. A Schematic diagram of establishing a hepatic lymphoma model in WT mice and FGF21KO mice. The mice were fed with HFMCD or CD for 2 weeks, then orthotopic inoculation was performed by EL4 cell injection in the liver lobe. Arrowhead: tumor nodules. **B** The gross anatomy of tumor nodules, histology by H&E staining, and proliferation by PCNA IHC staining in tumor/liver tissues from four experimental groups (WT-CD, WT-HFMCD, FGF21KO-CD, and FGF21KO-HFMCD). **C** Numbers of tumor nodules were counted macroscopically in the liver lobs from four experimental groups. **D** Computer-imaging analysis in IHC slides to calculate the indexes of PCNA positive cells from four experimental groups. **E** Immunofluorescent staining using the antibodies of anti-CD3 and anti-CD133 to detect EL4 cell growth in the tumor tissue from a FGF21KO-MASH-lymphoma mouse. **F** Analysis of extranodal infiltration (Ex) in stomach, lung, spleen, and skin from four experimental groups. **G**, **H** Western blotting analysis to detect the protein levels of β-catenin and EpCAM in the liver tissues from four experimental groups. Animal number (n) = 6 in each group; 21KO: FGF21KO.

21KD cells (Fig. S3). We speculated that FL83B-21KD cells (hepatocytes lacking FGF21) were unable to control abnormal lipid metabolism, while an overabundance of FAs has the potential to mediate the activation of Wnt/β-catenin and EpCAM signaling in EL4 cells (lymphoma cells). Taken together, aggressive growth of EL4 cells were found in the liver parenchyma of FGF21KO-MASH-lymphoma mice, coupled with the activation of Wnt/β-catenin and EpCAM signaling. A lack of FGF21 worsened lipid metabolic disorder in the hepatic microenvironment which further promoted lymphoma cell growth in the MASH liver.

Wnt/β-catenin signaling promoted EL4 cell growth via FGF21 mediated cross-talking

Canonical Wnt signaling is mainly mediated by β-catenin, whose degradation is controlled by a complex consisting of APC, axis inhibitor (AXIN), casein kinase 1 (CK1), and GSK-3β [31]. To determine the mechanisms of the Wnt/β-catenin signal transduction pathway, XAV939, an inhibitor of tankyrase activity, was used to stabilize AXIN thereby enhancing the degradation of β-catenin. Additionally, lithium chloride (LiCl), an inhibitor of GSK-3β, was used to induce phosphorylation of GSK-3β at ser9, leading to the accumulation of β-catenin and nuclear translocation thereby activating Wnt/β-catenin signaling. When EL4 cells were challenged with OP and subsequently treated with 1 μM XAV939 for 16 h, there was a significant increase in AXIN-1 protein expression (Fig. 4A), CK1α phosphorolated β-catenin at thr41, and GSK-3β induced phosphorylation of β-catenin at ser45 (Fig. 4B). Consistent with the XAV939 treatment, the OP-challenged EL4 cells were treated with LiCl at different concentrations for 16 h. The results showed that 20 mM of LiCl treatment significantly increased phosphorylation of GSK-3β at ser9 (Fig. 4C) along with hypophosphorylation of β-catenin at ser45 (Fig. 4D). This finding encouraged us to further investigate cyclin D1, a responsive target gene of the β-catenin-LEF/TCF axis. As expected, the cyclin D1 protein levels were significantly reduced by XAV939 but rescued by LiCl (Fig. 4E), which was consistent with the result of colony growth of OP-challenged EL4 cells with treatments of XAV939 and LiCl (Fig. 4F). To investigate whether the lack of FGF21 could mediate β-catenin signaling in contribution to EL4 cell growth, a trans-well migration assay was performed to study the migratory ability of EL4 cells. There was a significant increase in migration ability when EL4 cells were co-cultured with the OP-challenged 21KD-FL83B cells (Fig. 4G), confirming the aggressive growth behavior of EL4 in an aberrant lipid microenvironment due to the lack of FGF21. Treatment with XAV939 significantly decreased cellular migration while treatment with LiCl significantly increased migration (Fig. 4G), indicating that the activation of Wnt/β-catenin could give rise to lymphomagenesis, thus promoting migration of EL4 cells. We next asked if alleviating lipid metabolic disorder by FGF21 could affect Wnt/β-catenin and EpCAM signaling in lymphoma cells. First, OP-challenged FL83B-21KD cells were treated with rhFGF21 and then stained with Oil-red O to determine lipid accumulation. The results indicated that increased lipid accumulation in OP-challenged FL83B-21KD cells was attenuated by rhFGF21treatment (Fig. S4), suggesting that FGF21 could alleviate lipid disorder. Next, protein levels of β-catenin, EpCAM, and cyclin D1 were measured in EL4 cells co-cultured with OP-challenged FL83B-21KD cells with/without rhFGF21treatment. The results indicated that the increased expressions of β-catenin, EpCAM, and cyclin D1 were attenuated by rhFGF21treatment (Fig. 4H–J). Taken together, activation of Wnt/β-catenin signaling promoted the growth and migration of OP-challenged EL4 cells. Alleviating the lipid accumulation by restoration of FGF21 in hepatocytes downregulated the Wnt signaling to inhibit EL4 cell growth.

Fenofibrate prevented EL4 cell infiltration in MASH liver

Fenofibrate, a PPAR-α agonist, has been widely used in the treatment of dyslipidemia and diabetes for decades [32]. As hepatic expression of FGF21 is regulated by PPARα, we therefore investigated the potential therapeutic effects of fenofibrate to reduce hepatic lymphoma infiltration in MASH-lymphoma mice. The MASH-lymphoma model was established as described in Fig. 3A and the animals were treated with fenofibrate (Fig. 5A). The macroscopic findings of tumor nodules (Fig. 5B) and histology by H&E staining confirmed lymphoma infiltration (Fig. 5C). Significantly less hepatic lymphoma nodules were found in the fenofibrate treatment arms compared to the untreated control mice (Fig. 5D). Significantly decreased NAS (Fig. 5E), hepatic lipid accumulation, liver tissue TG levels (Fig. S5A, B), and liver weight (Fig. S5C) were also found in the fenofibrate treatment arms. In fenofibrate treatment groups, the $TG^{high}Ex^{+}$ cases decreased from 43% to 14% in WT-MASH-lymphoma mice, and from 57% to 31% in FGF21KO-MASH-lymphoma mice (Fig. 5F), suggesting that fenofibrate treatment alleviated lymphoma infiltration in other organs. To determine whether fenofibrate's bioactivity could affect Wnt/β-catenin signaling, OP-challenged EL4 cells were treated with fenofibrate in combination of XAV939 and LiCl. EL4 cells challenged with OP and treated with LiCl experienced an increase in colony growth, however after the addition of fenofibrate, growth was inhibited (Fig. 5G), suggesting fenofibrate could block the Wnt/β-catenin signaling. Of note, fenofibrate had better therapeutic success in WT-MASH-lymphoma mice over FGF21KO-MASH-lymphoma mice, as evidenced by the decrease in hepatic lymphoma nodules, NAS, and Ex cases. In this respect, lymphoma suppression by fenofibrate could act via the PPAR-α-FGF21 axis to alleviate the burden of FFA. To test this notion, the serum FFA levels were measured in both the WT-MASH-lymphoma and FGF21KO-MASH-lymphoma mice. With fenofibrate treatment, serum FFA was significantly reduced in WT-MASH-lymphoma mice compared to FGF21KO-MASH-lymphoma mice (Fig. 5H). A significant increase in protein PPAR-α was found in both WT-MASH-lymphoma and FGF21KO-MASH-lymphoma mice, but the FGF21 protein was only detected in the WT-MASH-lymphoma mice (Fig. 5I), suggesting the existence of a fenofibrate-PPAR-α-FGF21 axis. Consistent with therapeutic efficacy, fenofibrate treatments significantly reduced β-catenin and EpCAM in the liver tissues from WT-MASH-lymphoma mice compared to FGF21KO-MASH-lymphoma mice (Fig. 5I). Collectively, these results suggest that the fenofibrate-PPAR-α-FGF21 axis is a negative feedback loop for both the alleviation of MASH and inhibition of Wnt/β-catenin signaling to prevent hepatic lymphoma infiltration.

Aberrant Wnt/β-catenin signaling and TG level in human T-cell lymphoma

The Wnt/β-catenin signal transduction pathway was further investigated in the human T-lymphoblastic lymphoma HH cells. Based on the XTT results (Fig. S6A), 0.5 mM OP was selected to treat the HH cells for 24 h. Consistent with our findings in mouse lymphoma cells (EL4), the protein expression of AXIN-1 was significantly up-regulated (Fig. 6A) along with increased phosphorylation of β-catenin at thr41 and ser45 (Fig. 6B). In addition, there was a significant increase in GSK-3β phosphorylation at ser9 (Fig. 6C) along with hypophosphorylation of β-catenin at ser45 (Fig. 6D). These results confirmed the activation of Wnt/β-catenin signal transduction pathways in human T-lymphoblastic lymphoma cells (HH) challenged with OP. The migratory ability of OP-challenged/LiCl-treated HH cells was attenuated by not only Wnt/β-catenin signaling inhibitor (XAV939) but also subsequently treated with fenofibrate in combinationn of XAV939 (Fig. 6E), suggesting that fenofibrate could further block the Wnt/β-catenin signaling pathway in human T-lymphoblastic lymphoma cells. A retrospective analysis was performed to evaluate hypertriglyceridemia (TG level ≥ 1.8 mmol/L) in a cohort of 257 peripheral T-cell lymphoma (PTCL) patients with and without extranodal infiltration (Ex). The PTCL patients with Ex showed hypertriglyceridemia compared to PTCL patients without Ex, with statical significance

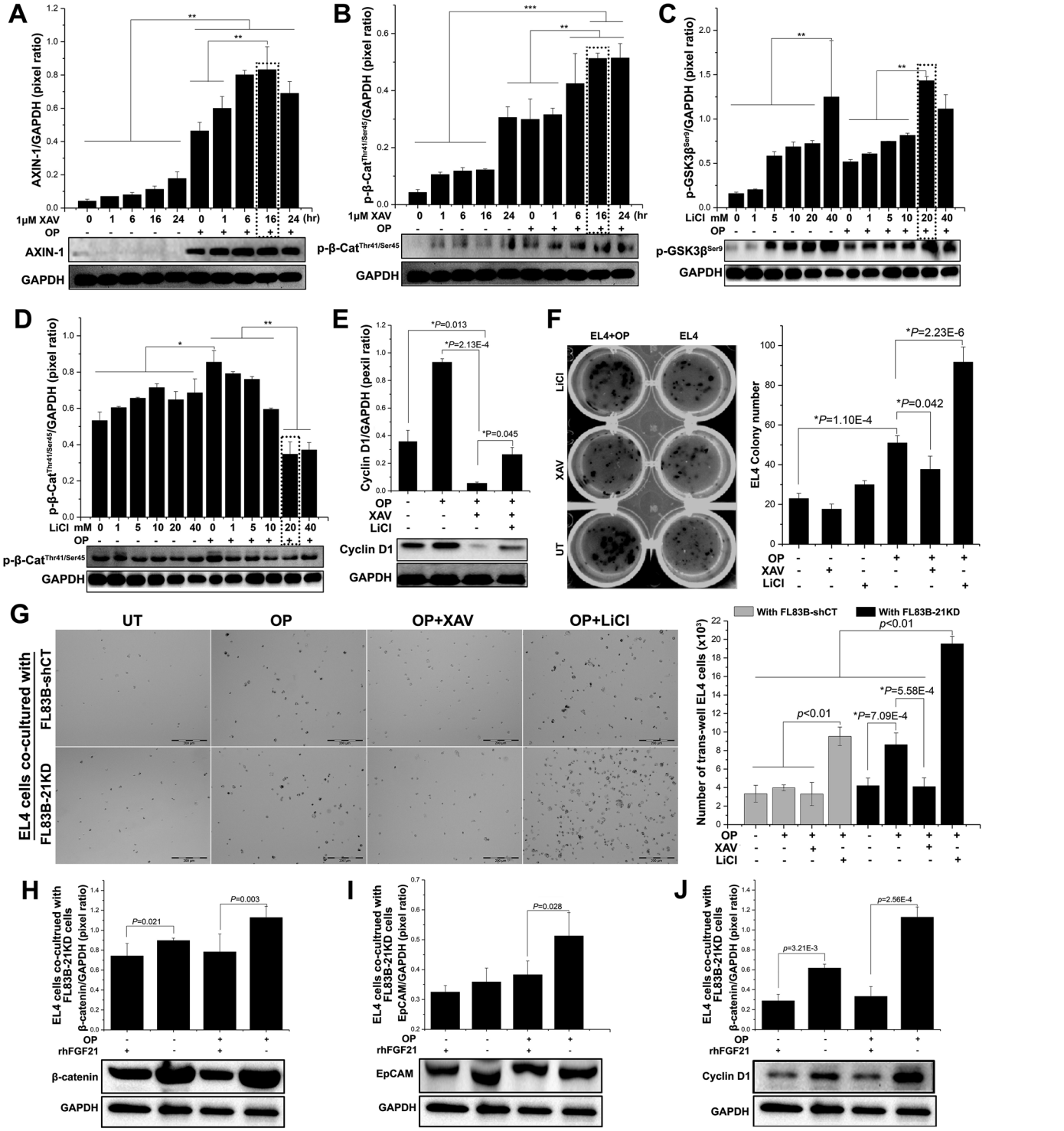

Fig. 4 Wnt/β-catenin signaling promoted EL4 cell growth. A, **B** Western blot analysis for protein levels of AXIN-1 and phosphorylated β-catenin at thr41/ser45 from the OP-challenged EL4 cells treated with 1 μM XAV939 treatment at different time points, up to 24 h. **C**, **D** Western blot analysis for protein levels of phosphorylated GSK-3β at ser9 and phosphorylated β-catenin at thr41/ser45 from the OP-challenged EL4 cells treated with LiCl at different concentrations for 16 h. **E** Western blot analysis for protein levels of cyclin D1 from the OP-challenged EL4 cells treated with 20 mM LiCl and 1 μM XAV939 for 16 h. **F** Colony forming assay to detect the number of OP-challenged EL4 cells treated with 20 mM LiCl and 1 μM XAV939 for 16 h. **G** Trans-well assay to determine the migratory ability of EL4 cells co-cultured with OP-challenged FL83B-21KD cells or with OP-challenged FL83B-shCT cells, which were treated with 20 mM LiCl and/or 1 μM XAV939 for 16 h. **H–J** Western blot analysis for protein levels of β-catenin, EpCAM, and cyclin D1 from the EL4 cells co-cultured OP-challenged FL83B-21KD cells or with OP-challenged FL83B-shCT cells, which were treated with rhFGF21 at 100 ng/mL. OP: a mixture of oleic acid and palmitic acid (2:1); XAV: XAV939; p-β-Cat: phosphorylated β-catenin; p-GSK-3β: phosphorylated GSK-3β.

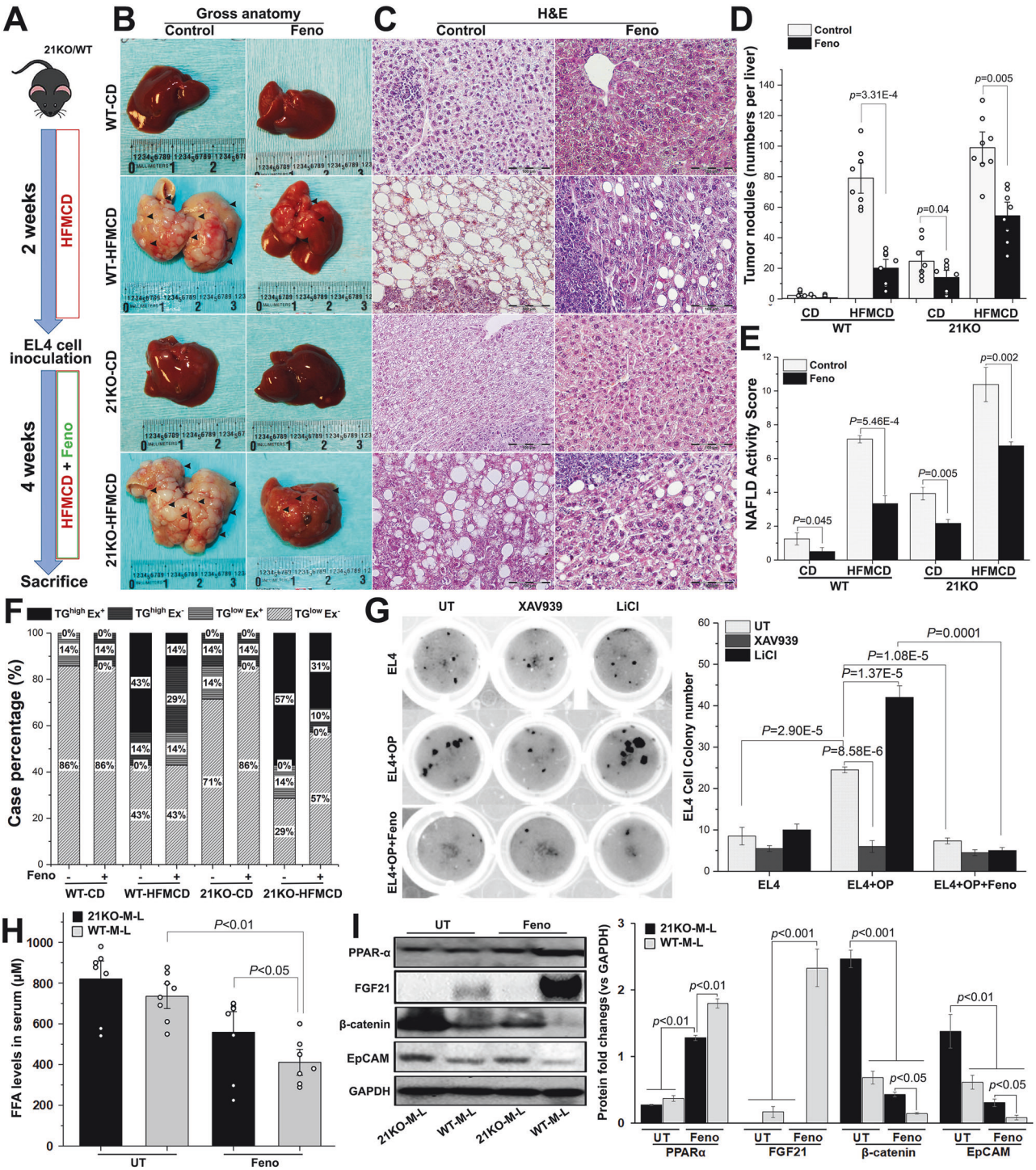

Fig. 5 Fenofibrate prevented EL4 cell infiltration in MASH liver. A Schematic diagram of establishing the hepatic lymphoma model and fenofibrate treatment in WT mice and FGF21KO mice. **B** The gross anatomy of tumor nodules from the experimental groups (WT-CD, WT-HFMCD, FGF21KO-CD, and FGF21KO-HFMCD) with/without fenofibrate treatment. Arrowhead: tumor nodules. **C** The representative images of histology by H&E in the liver/tumor tissues from the experimental groups. **D** Numbers of tumor nodules were counted macroscopically in the liver lobs from the experimental groups. **E** Histology based NAFLD activity score (NAS) from the experimental groups. **F** Analysis of extranodal infiltration (Ex) in stomach, lung, spleen, and skin from the experimental groups. **G** Colony forming assay to detect the number of cell colonies of OP-challenged EL4 cells treated with 20 mM LiCl, 1 μM XAV939, and 100 μM fenofibrate for 16 h. **H** Serum FFA levels in the WT-MASH-lymphoma mice and FGF21KO-MASH-lymphoma mice with/without fenofibrate treatment. Western blot analysis to detect the protein levels of PPAR-α, FGF21, β-catenin and EpCAM in the liver tissues from WT-MASH-lymphoma mice and FGF21KO-MASH-lymphoma mice with/without fenofibrate treatment. OP: a mixture of oleic acid and palmitic acid (2:1); Animal number (n) = 8 in each group; 21KO: FGF21KO; XAV: XAV939; UT: untreated; Feno: fenofibrate. WT-M-L: WT-MASH-lymphoma; 21KO-M-L: FGF21KO-MASH-lymphoma.

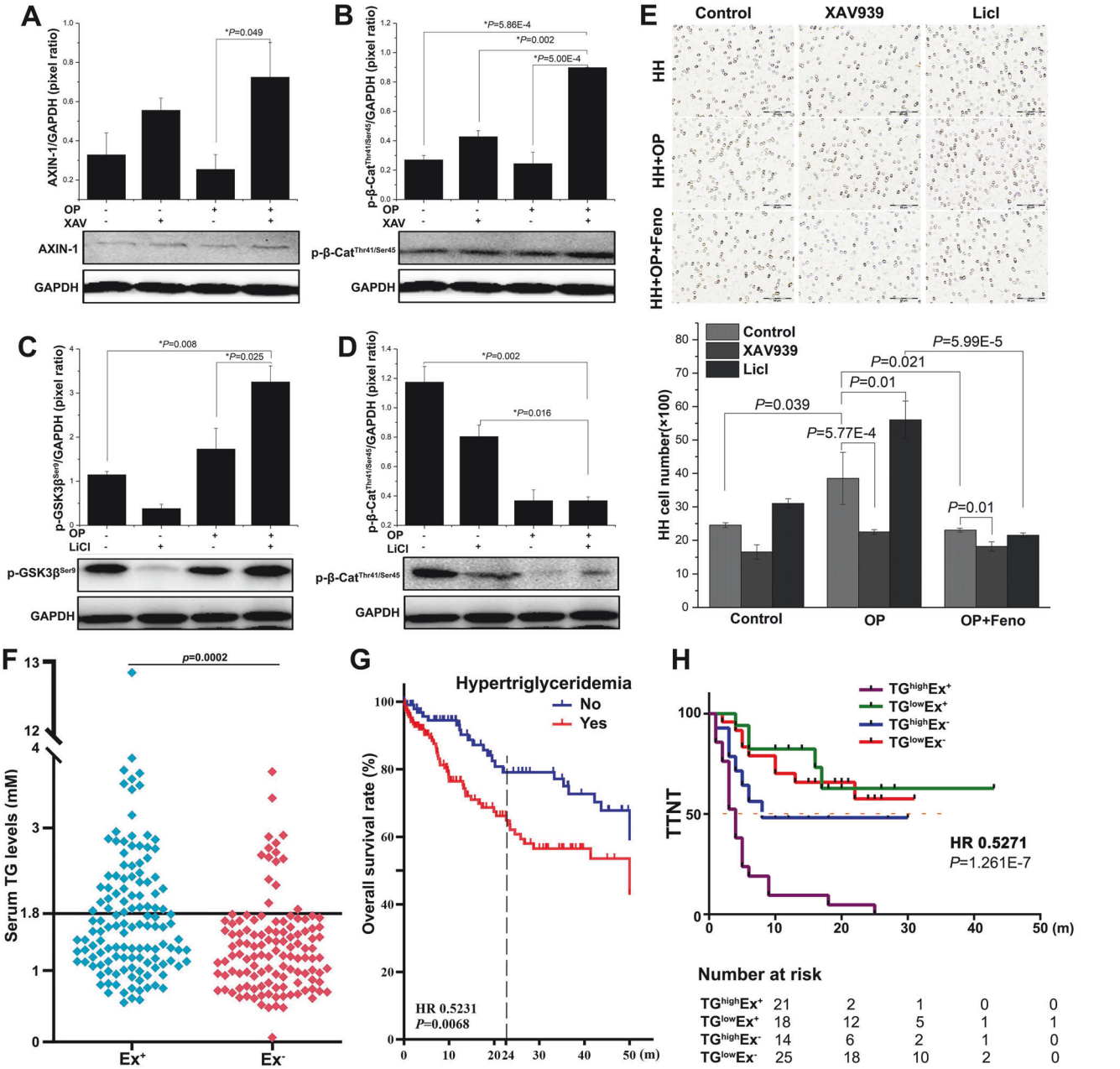

Fig. 6 Aberrant Wnt/β-catenin signaling in human T-lymphoblastic lymphoma, and TG level associated survival and Ex in PTCL patients. **A**, **B** Western blot analysis of AXIN-1 and phosphorylated β-catenin at thr41/ser45 from the OP-challenged HH cells treated with 1 μM XAV939 treatment for 16 h. **C**, **D** Western blot analysis of phosphorylated GSK-3β at ser9 and phosphorylated β-catenin at thr41/ser45 from the OP-challenged HH cells treated with 20 mM LiCl for 16 h. **E** Trans-well assay to determine the migratory ability of HH cells which were challenged with OP and treated with 20 mM LiCl and 1 μM XAV939 for 16 h. OP: a mixture of oleic acid and palmitic acid (2:1); p-β-Cat: phosphorylated β-catenin; p-GSK-3β: phosphorylated GSK-3β; Ex: extranodal lymphoma. **F** Serum TG levels in the PTCL patients with/without Ex. **G** Kaplan–Meier plot of overall survival in the PTCL patients diagnozed hypertriglyceridemia (TG level ≥1.8 mmol/L) compared to the patients with normal serum TG levels. Black dash: 24 months. **H** Kaplan–Meier plot of time to next anti-lymphoma treatment (TTNT) in PTCL patients with/without extranodal lymphoma and with/without hypertriglyceridemia. Orange dash in (**H**): median TTNT.

(Fig. 6F). The overall survival (OS) and time to next anti-lymphoma treatment (TTNT) were calculated and the 2-year OS rate of patients without hypertriglyceridemia showed 79.1%, significantly higher than the 2-year OS rate (62.1%) in patients with hyperlipidemia (Fig. 6G). Seventy-eight PTCL patients finished 4 cycles of CHOP (cyclophosphamide, doxorubicin, vincristine, and prednisone) therapy and were followed for 50 months. In this cohort, the patients with hypertriglyceridemia were grouped into TG^{high}, and the rest patients were placed into TG^{low} to elucidate TTNT in patients with/without Ex. The median TTNT in the $TG^{high}Ex^{+}$ patients was less than 3 months, which was significantly less than the median TTNT in the $TG^{low}Ex^{+}$, $TG^{high}Ex^{-}$, and $TG^{low}Ex^{-}$ patients (Fig. 6H and Fig. S6B–D). Taken together, OP-challenging in human T-lymphoblastic lymphoma cells caused activation of Wnt/β-catenin signaling. Fenofibrate suppressed the migratory ability of HH cells via Wnt/β-catenin signaling blockage, in addition to alleviating aberrant lipid metabolism. Hypertriglyceridemia is negatively associated with the overall survival rate in PTCL patients, and PTCL patients with hypertriglyceridemia could be at high risk of extranodal infiltration.

DISCUSSION

Activation of Wnt/β-catenin signaling in lymphoma has been previously reported [33], however, its relation to lymphomagenesis was mostly focused on DLBCL, despite a wide variety of lymphoma entities [33]. Here, we report for first time that the activation of Wnt/β-catenin signaling pathway contributed to aggressive growth of T-lymphoblastic lymphoma. We found the increased protein levels of β-catenin and EpCAM in mouse/human T-lymphoblastic lymphoma cells challenged with FA. In our established MASH-lymphoma model engrafted with EL4 cells, we found a significant increase of β-catenin and EpCAM in tumor nodules compared to benign adjacent tissues. A characteristic feature of the canonical Wnt/β-catenin signaling pathway is to tightly regulate β-catenin levels via CK1- and GSK-3β-mediated phosphorylation [31]. With XAV939 treatment, the decreased cyclin D1 levels in the setting of phosphorylation of β-catenin at thr41 (CK1-mediated) and at ser45 (GSK-3β-mediated) confirmed the involvement of the Wnt/β-catenin signaling cascade contributing to aggressive growth of T-lymphoblastic lymphoma. Although there is no previous study to investigate the Wnt/β-catenin signaling pathway in T-lymphoblastic lymphoma, the Wnt/β-catenin pathway has been found to promote, (1) early engraftment of fetal hematopoietic stem/progenitor cells [34], (2) aggressive growth of T-cell acute lymphoblastic leukemia [35], and (3) proliferation of DLBCL [36]. Our findings agreed with those studies mentioned above. In addition, both EL4 cells [37] and hepatocytes [38] can release exosomes which carry functional lipids and mediate cell cross-talking. The exosome-mediated lipid transfer from hepatocytes to EL4 cells caused an increase in lipid accumulation, which can also play an important role contributing to Wnt/β-catenin activation [39]. Of note, AXIN is a structural scaffold protein in regulating not only Wnt/β-catenin pathway but also lipid metabolism. A study showed that the inhibited glucose production and the reduced lipogenesis by pyrvinium in hepatocytes were partially elicited by the downregulation of β-catenin through AXIN stabilization [40]. In our study, we found that OP treatment could induce AXIN production in EL4 cells. It is of great interest to further study the role of AXIN in cellular lipid homeostasis which influences the cell growth of T-lymphoblastic lymphoma.

Metabolic reprogramming of lipid metabolism has been accepted as playing a critical role in carcinogenesis of various human malignancies [41], but it is disregarded somehow in lymphoma research. Hypertriglyceridemia was noted in a transplanted hamster lymphoma in the 1970s [42, 43], however, the aberrant lipid metabolism in lymphomas has remained largely unexplored. In this study, we found aggressive infiltration of EL4 cells in the liver parenchyma of established MASH-lymphoma mice, coupled with Wnt/β-catenin and EpCAM signaling activation. The knockout of FGF21 worsened lipid dysfunction which further promoted lymphoma cell growth in the MASH liver. Fenofibrate treatment suppressed lymphoma infiltration which could be dependent on both PPAR-α induced FGF21 induction to alleviate aberrant FA metabolism and inhibition of Wnt/β-catenin signaling. Our findings are supported by the following previous studies: 1) aberrant FA signaling mediated activation of Wnt/β-catenin signaling in various cancers such as cervical cancer and colon cancer [44, 45]; 2) FGF21 protected the liver against MASH via clearance of excessive FFAs thereby negatively regulating steatosis [12, 13, 16]; 3) FGF21 suppressed HCC initiation and HCC metastasis by inhibiting β-catenin signaling [14, 15, 46]; (4) fenofibrate upregulated gene expression of FGF21 in hepatocytes via PPAR-α, thereby prevented MASH and inhibited β-catenin signaling [22]; (5) fenofibrate could directly induce apoptosis in human and mouse lymphoma cells [47]; (6) fenofibrate downregulated kallistatin, a well-known suppressor of the GSK-3β/β-catenin signaling pathway, to prevent MASH [48]. Our data suggested that fenofibrate could be an effective therapy against lymphomagenesis of extranodal infiltration, particularly in metabolically compromised organs such as MASH liver.

In conclusion, aberrant lipid metabolism contributed to the aggressive growth of T-lymphoblastic lymphoma cells in MASH liver. Wnt/β-catenin signaling could be a potential lymphomagenetic mechanism for extranodal infiltration of T-lymphoblastic lymphoma. Fenofibrate has the potential to be an effective therapeutic strategy against liver infiltration of T-lymphoblastic lymphoma in MASH liver.

REFERENCES

1. Masood A, Kairouz S, Hudhud KH, Hegazi AZ, Banu A, Gupta NC. Primary non-Hodgkin lymphoma of liver. Curr Oncol. 2009;16:74–77.
2. Gherlan GS, Stoia R, Enyedi M, Dobrea C, Calistru PI. Primary hepatic marginal zone lymphoma in a patient with chronic hepatitis C. Maedica (Buchar). 2016;11:250–4.
3. Bao C, Wei J, Zhao X, Lin L, Chen D, Liu K, et al. Prognostic value of fluorine-18-fluorodeoxyglucose positron emission tomography/computed tomography in primary hepatic mucosa-associated lymphoid tissue lymphoma: a case report and review of the literature. Med (Balt). 2018;97:e9877.
4. Dong S, Chen L, Chen Y, Chen X. Primary hepatic extranodal marginal zone B-cell lymphoma of mucosa-associated lymphoid tissue type: a case report and literature review. Med (Balt). 2017;96:e6305.
5. Baumhoer D, Tzankov A, Dirnhofer S, Tornillo L, Terracciano LM. Patterns of liver infiltration in lymphoproliferative disease. Histopathology. 2008;53:81–90.
6. Shigematsu A, Okada K, Abe N, Ota S, Kato N, Kondo K, et al. Non-alcoholic steatohepatitis occurring in a patient with T-lymphoblastic lymphoma during chemotherapy including prednisolone. Leuk Lymphoma. 2006;47:1397–9.
7. Kose D, Erol C, Kaya F, Koplay M, Koksal Y. Development of fatty liver in children with non-Hodgkin lymphoma. Turk J Pediatr. 2014;56:399–403.
8. Kosmidou IS, Aggarwal A, Ross JJ, Worthington MG. Hodgkin' s disease with fulminant non-alcoholic steatohepatitis. Dig Liver Dis. 2004;36:691–3.
9. Peters AM, Keramida G, Pencharz D. Assessment of alteration in liver (18)F-FDG uptake due to steatosis in lymphoma patients and its impact on the Deauville score. Eur J Nucl Med Mol Imaging. 2018;45:2231–2.
10. Frenquelli M, Tonon G. WNT signaling in hematological malignancies. Front Oncol. 2020;10:615190.
11. Bugter JM, Fenderico N, Maurice MM. Mutations and mechanisms of WNT pathway tumour suppressors in cancer. Nat Rev Cancer. 2021;21:5–21.
12. Talukdar S, Kharitonenkov A. FGF19 and FGF21: In NASH we trust. Mol Metab. 2021;46:101152.
13. Inagaki T, Dutchak P, Zhao G, Ding X, Gautron L, Parameswara V, et al. Endocrine regulation of the fasting response by PPARalpha-mediated induction of fibroblast growth factor 21. Cell Metab. 2007;5:415–25.
14. Liu X, Zhang P, Martin RC, Cui G, Wang G, Tan Y, et al. Lack of fibroblast growth factor 21 accelerates metabolic liver injury characterized by steatohepatities in mice. Am J Cancer Res. 2016;6:1011–25.
15. Zhang Q, Li Y, Liang T, Lu X, Liu X, Zhang C, et al. Loss of FGF21 in diabetic mouse during hepatocellular carcinogenetic transformation. Am J Cancer Res. 2015;5:1762–74.
16. Fisher FM, Maratos-Flier E. Understanding the physiology of FGF21. Annu Rev Physiol. 2016;78:223–41.
17. Cross AJ, Lim U. The role of dietary factors in the epidemiology of non-Hodgkin's lymphoma. Leuk Lymphoma. 2006;47:2477–87.
18. Wang X, Guo W, Shi X, Chen Y, Yu Y, Du B, et al. S1PR1/S1PR3-YAP signaling and S1P-ALOX15 signaling contribute to an aggressive behavior in obesity-lymphoma. J Exp Clin Cancer Res. 2023;42:3.
19. Wai CMM, Chen S, Phyu T, Fan S, Leong SM, Zheng W, et al. Immune pathway upregulation and lower genomic instability distinguish EBV-positive nodal T/NK-cell lymphoma from ENKTL and PTCL-NOS. Haematologica. 2022;107:1864–79.
20. Qin BB, Tang DF, Ni ML, Gao W, Zhang MZ. The aberrant activation of Wnt pathway caused by beta-catenin mutation and its prognostic significance in NK/T-cell lymphoma. Neoplasma. 2019;66:20–27.
21. Chiarini F, Paganelli F, Martelli AM, Evangelisti C. The role played by Wnt/beta-catenin signaling pathway in acute lymphoblastic leukemia. Int J Mol Sci. 2020;21:1098.
22. Galman C, Lundasen T, Kharitonenkov A, Bina HA, Eriksson M, Hafstrom I, et al. The circulating metabolic regulator FGF21 is induced by prolonged fasting and PPARalpha activation in man. Cell Metab. 2008;8:169–74.
23. Tan Y, Wang M, Yang K, Chi T, Liao Z, Wei P. PPAR-alpha Modulators as Current and Potential Cancer Treatments. Front Oncol. 2021;11:599995.
24. Hayes CN, Zhang P, Chayama K. The Role of Lipids in Hepatocellular Carcinoma. In: Tirnitz-Parker JEE (ed). Hepatocellular Carcinoma: Brisbane (AU), 2019.

25. Pandit H, Li Y, Li X, Zhang W, Li S, Martin RCG. Enrichment of cancer stem cells via beta-catenin contributing to the tumorigenesis of hepatocellular carcinoma. BMC Cancer. 2018;18:783.
26. Zhang Y, Wang X. Targeting the Wnt/beta-catenin signaling pathway in cancer. J Hematol Oncol. 2020;13:165.
27. Zheng Q, Martin RC, Shi X, Pandit H, Yu Y, Liu X, et al. Lack of FGF21 promotes NASH-HCC transition via hepatocyte-TLR4-IL-17A signaling. Theranostics. 2020;10:9923–36.
28. Brunt EM, Kleiner DE, Wilson LA, Belt P, Neuschwander-Tetri BA. Network NCR. Nonalcoholic fatty liver disease (NAFLD) activity score and the histopathologic diagnosis in NAFLD: distinct clinicopathologic meanings. Hepatology. 2011;53:810–20.
29. Cariello M, Moschetta A. Fibroblast growth factor 21: a new liver safeguard. Hepatology. 2014;60:792–4.
30. Henriksson E, Andersen B. FGF19 and FGF21 for the treatment of NASH-two sides of the same coin? differential and overlapping effects of FGF19 and FGF21 from mice to human. Front Endocrinol (Lausanne). 2020;11:601349.
31. Albrecht LV, Tejeda-Munoz N, De Robertis EM. Cell biology of canonical Wnt signaling. Annu Rev Cell Dev Biol. 2021;37:369–89.
32. Balfour JA, McTavish D, Heel RC. Fenofibrate. A review of its pharmacodynamic and pharmacokinetic properties and therapeutic use in dyslipidaemia. Drugs. 1990;40:260–90.
33. Yu S, Han R, Gan R. The Wnt/beta-catenin signalling pathway in Haematological Neoplasms. Biomark Res. 2022;10:74.
34. Kwarteng EO, Hetu-Arbour R, Heinonen KM. Frontline Science: Wnt/beta-catenin pathway promotes early engraftment of fetal hematopoietic stem/progenitor cells. J Leukoc Biol. 2018;103:381–93.
35. Evangelisti C, Chiarini F, Cappellini A, Paganelli F, Fini M, Santi S, et al. Targeting Wnt/beta-catenin and PI3K/Akt/mTOR pathways in T-cell acute lymphoblastic leukemia. J Cell Physiol. 2020;235:5413–28.
36. Zhao CC, Jiao Y, Zhang YY, Ning J, Zhang YR, Xu J, et al. Lnc SMAD5-AS1 as ceRNA inhibit proliferation of diffuse large B cell lymphoma via Wnt/beta-catenin pathway by sponging miR-135b-5p to elevate expression of APC. Cell Death Dis. 2019;10:252.
37. Tavakkoli S, Sotoodehnejadnematalahi F, Fathollahi A, Bandehpour M, Haji Molla Hoseini M, Yeganeh F. EL4-derived exosomes carry functional TNF-related apoptosis-inducing ligand that are able to induce apoptosis and necrosis in the target cells. Int J Mol Cell Med. 2020;9:207–15.
38. Xu W, Mo W, Han D, Dai W, Xu X, Li J, et al. Hepatocyte-derived exosomes deliver the lncRNA CYTOR to hepatic stellate cells and promote liver fibrosis. J Cell Mol Med. 2024;28:e18234.
39. Lu F, Ye M, Hu C, Chen J, Yan L, Gu D, et al. FABP5 regulates lipid metabolism to facilitate pancreatic neuroendocrine neoplasms progression via FASN mediated Wnt/beta-catenin pathway. Cancer Sci. 2023;114:3553–67.
40. Zhou S, Obianom ON, Huang J, Guo D, Yang H, Li Q, et al. Pyrvinium treatment confers hepatic metabolic benefits via beta-catenin downregulation and AMPK activation. Pharmaceutics. 2021;13:330.
41. Liu Q, Luo Q, Halim A, Song G. Targeting lipid metabolism of cancer cells: a promising therapeutic strategy for cancer. Cancer Lett. 2017;401:39–45.
42. Beaumont V, Berard M, Boisnier C, Beaumont JL. [Hyperlipemia and tumors : post heparin lipase activity of the hamster bearing a malignant lymphoma]. C R Acad Hebd Seances Acad Sci D. 1975;280:665–8.
43. Beaumont JL, Beaumont V, Boisnier C, Szondy E, Vranckx R. [Antiheparin immunoglobulin in malignant lymphoma with hypertriglyceridemia, in the hamster]. C R Acad Hebd Seances Acad Sci D. 1976;283:1369–72.
44. Kumar SS, Fathima A, Srihari P, Jamma T. Host-gut microbiota derived secondary metabolite mediated regulation of Wnt/beta-catenin pathway: a potential therapeutic axis in IBD and CRC. Front Oncol. 2024;14:1392565.
45. Liu H, Liu Y, Zhou Y, Chen X, Pan S, Zhou Q, et al. TM7SF2-induced lipid reprogramming promotes cell proliferation and migration via CPT1A/Wnt/beta-Catenin axis in cervical cancer cells. Cell Death Discov. 2024;10:207.
46. Xia J, Zhu Z, Wen G, Chen Y, An R, Xia S, et al. Aberrant acetylated modification of FGF21-KLB signaling contributes to hepatocellular carcinoma metastasis through the beta-catenin pathway. Int J Oncol. 2023;63:91.
47. Schmeel LC, Schmeel FC, Schmidt-Wolf IGH. In vitro apoptosis induction by fenofibrate in lymphoma and multiple myeloma. Anticancer Res. 2017;37:3513–20.
48. Fang Z, Shen G, Wang Y, Hong F, Tang X, Zeng Y, et al. Elevated Kallistatin promotes the occurrence and progression of non-alcoholic fatty liver disease. Signal Transduct Target Ther. 2024;9:66.

AUTHOR CONTRIBUTIONS

WG worked on retrospective analysis of serum TG, overall survival, and TTNT in the cohort of 257 PTCL patients. WG and XW worked on serum FFA measurements, IHC, Flow cytometry, Western blot, qPCR, and data analysis. GC and WG worked on animal models. BZ and WG worked on the lymphomas data analysis on the dataset (GSE160119) which was sourced from the NCBI GEO database. ES and YG assisted partly data analysis. WG and YL worked on experimental design and manuscript draft. RM and OB contributed to clinical consulting. ES and YL contributed to manuscript English checking. All the authors read and approved the final manuscript.

FUNDING

Research reported in this publication was supported partly by Natural Science Foundation of Jilin Province (20210101432JC).

COMPETING INTERESTS

The authors declare that they have no competing interests. All human procedures for this study were approved (#2021-680) by the Institutional Review Board for Human Study at The First Hospital of Jilin University, and all informed consent paperwork was properly obtained. All animal procedures were approved (#19528) by the Institutional Animal Care and Use Committee of the University of Louisville, which is certified by the American Association for Accreditation of Laboratory Animal Care.

ADDITIONAL INFORMATION

Supplementary information The online version contains supplementary material available at https://doi.org/10.1038/s41388-025-03630-7.

Correspondence and requests for materials should be addressed to Ou Bai or Yan Li.